Supplementary Material for Observation of a Charge-2 Photonic Weyl Point in the Infrared

Sachin Vaidya[1*], Jiho Noh[1*], Alexander Cerjan[1], Christina Jörg[1,2], Georg von Freymann[2,3], Mikael C. Rechtsman[1]
[1] *Department of Physics, The Pennsylvania State University, University Park, PA 16802, USA*
[2] *Physics Department and Research Center OPTIMAS, Technische Universitt Kaiserslautern, 67663 Kaiserslautern, Germany,*
[3] *Fraunhofer Institute for Industrial Mathematics ITWM, 67663 Kaiserslautern, Germany*

BAND STRUCTURE

The full 3D band structure for the chiral woodpile structure discussed in the main text is plotted in Fig. S1 (a). The two bands that make up the Weyl point are well-separated in frequency along the $\mathbf{Y}-\mathbf{\Gamma}-\mathbf{X}$ directions but are very close in frequency along $\mathbf{\Gamma}-\mathbf{Z}$. We perform convergence tests in MPB that confirm that the degeneracy only occurs at $\mathbf{\Gamma}$. This structure also has a charge -2 Weyl point at $\mathbf{R}$ between bands 3 and 4 which lies below the light line of air. Fig. S1 (b) shows the band structure for the same structure but with $\varepsilon_{\text{rods}} = 12$. The charge ± 2 Weyl points remain at $\mathbf{\Gamma}$ and $\mathbf{R}$ points of the Brillouin zone, protected by screw symmetry.

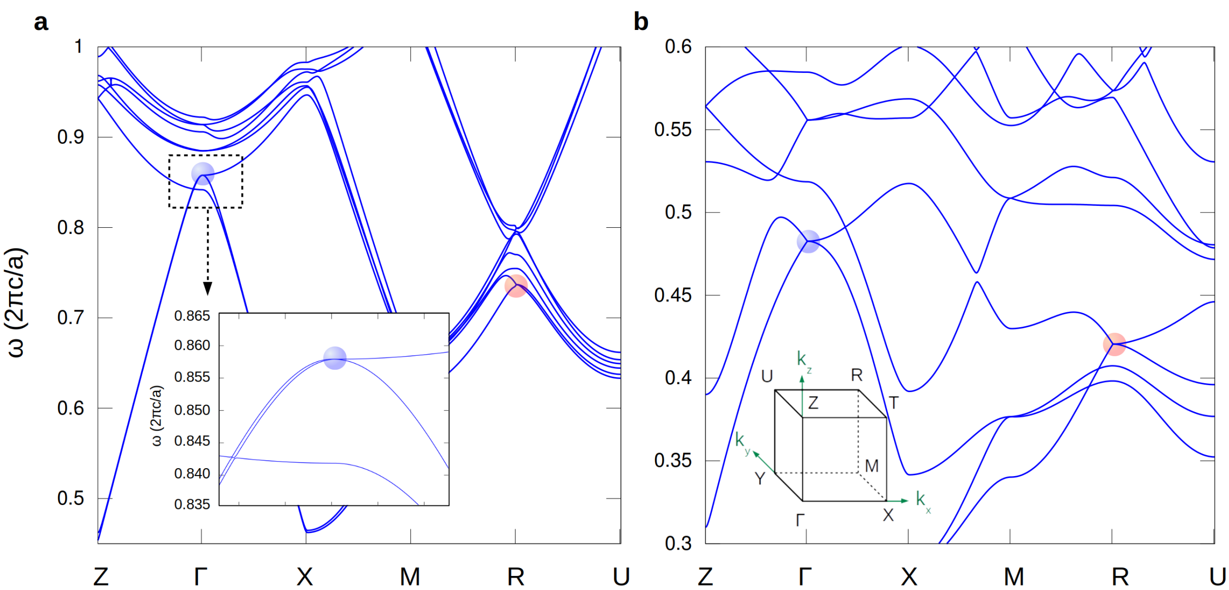

FIG. S1. (a) The full band structure for the PhC fabricated in the experiment with the following parameters: dielectric constant of rods ($\varepsilon_{\text{rods}}$) $= 2.31$, rod width (w) $= 0.175a$ and rod height (h) $= 0.25a$, where a is the lattice constant in all three directions. The inset contains the bands in the vicinity of $\mathbf{\Gamma}$. The charge ± 2 Weyl points are marked with a blue and red circle respectively. (b) Band structure showing bands 1 to 8 of the PhC for the same values of w and h but $\varepsilon_{\text{rods}} = 12$.

CALCULATION OF BERRY PHASE

As discussed in the main text, we numerically calculate the topological charge (Chern number) associated with the Weyl points at $\mathbf{\Gamma}$ and $\mathbf{R}$ of the chiral woodpile PhC. Here we describe that algorithm, following Ref. [1]. Consider a closed contour C in momentum ($\mathbf{k}$) space discretized into N points ($\mathbf{k_1}, ..., \mathbf{k_{N-1}}$) such that $\mathbf{k_N} = \mathbf{k_1}$. The total

---

* These authors contributed equally to this work

phase acquired by a state undergoing adiabatic transport along this loop is numerically calculated by

$$\theta_B(C) = -\mathrm{Im}\ln\left(\prod_{i=1}^{N}\frac{\langle\psi(\mathbf{k_i})|\psi(\mathbf{k_{i+1}})\rangle}{|\langle\psi(\mathbf{k_i})|\psi(\mathbf{k_{i+1}})\rangle|}\right) \tag{S1}$$

$\theta_B(C)$ is a manifestly gauge-invariant quantity and is called the Berry phase. In our case, the states in a 3D PhC are magnetic field eigenmodes of the Maxwell operator [2] that satisfy

$$\nabla\times\left(\frac{1}{\varepsilon(\mathbf{r})}\nabla\times\mathbf{H}(\mathbf{r})\right) = \left(\frac{\omega}{c}\right)^2\mathbf{H}(\mathbf{r}) \tag{S2}$$

and the inner product between two such eigenmodes is defined as

$$\langle\psi_1|\psi_2\rangle = \int \mathbf{H}_1^*(\mathbf{r})\cdot\mathbf{H}_2(\mathbf{r})\mathrm{d}^3\mathbf{r} \tag{S3}$$

This phase is calculated on circular contours that lie on constant k_z planes as shown in Fig. S2 (b). The topological charge of the Weyl point is the number of times the Berry phase winds as a function of k_z.

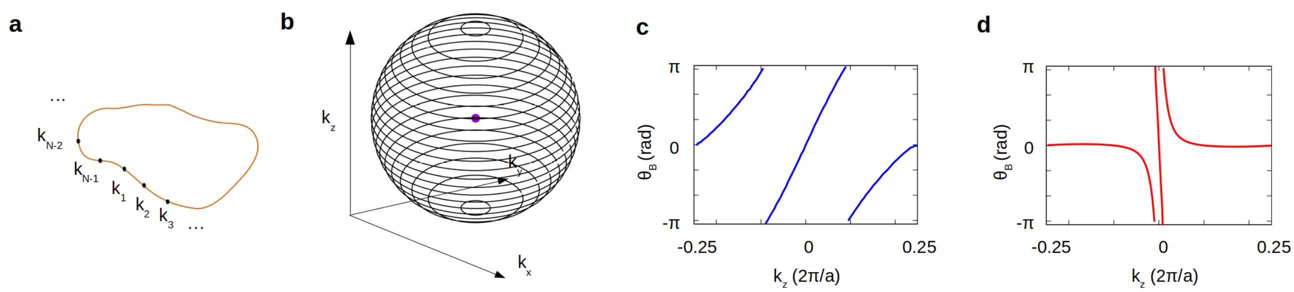

FIG. S2. (a) Closed contours in k-space discretized into N points. (b) The Berry phase is calculated on circular contours that enclose the Weyl point. Each contour lies on a constant k_z plane. (c), (d) Berry phase vs. k_z plots for charge +2 and charge −2 Weyl points at $\mathbf{\Gamma}$ and $\mathbf{R}$ respectively.

To show that the Weyl points are indeed symmetry protected and continue to exist even at low contrast, we start with a high contrast version of our PhC and plot the band structure and Berry phase as the contrast is smoothly lowered. An animated version of these plots can be found in the supplementary material.

COUPLING COEFFICIENTS BETWEEN INCIDENT PLANE WAVES AND PHC BLOCH MODES

To understand the relationship between the observed spectral features and the bulk bands, we calculate coefficients that measure the polarization of Bloch modes. For this, we consider plane waves with s- and p- polarizations incident along the $\mathbf{\Gamma}-\mathbf{X}$ direction on the PhC-air interface and define the polarization coupling coefficients C_s and C_p and mode coupling index κ [3–6]

$$\eta_{p,\mathbf{k},n} = \frac{\left|\iiint \hat{\mathbf{y}}\cdot\mathbf{H}_{\mathbf{k},n}(x,y,z)\mathrm{dxdydz}\right|^2}{V\iiint\left|\mathbf{H}_{\mathbf{k},n}(x,y,z)\right|^2\mathrm{dxdydz}} \tag{1}$$

$$\eta_{s,\mathbf{k},n} = \frac{\left|\iiint(\cos\theta\hat{\mathbf{x}}-\sin\theta\hat{\mathbf{z}})\cdot\mathbf{H}_{\mathbf{k},n}(x,y,z)\mathrm{dxdydz}\right|^2}{V\iiint|\mathbf{H}_{\mathbf{k},n}(x,y,z)|^2\mathrm{dxdydz}} \tag{2}$$

$$\kappa = \eta_{s,\mathbf{k},n}+\eta_{p,\mathbf{k},n};\quad C_{s/p} = \frac{\eta_{s/p,\mathbf{k},n}}{\kappa} \tag{3}$$

where $\mathbf{H}_{\mathbf{k},n}(x,y,z)$ is the magnetic field eigenmode of the PhC with momentum $\mathbf{k}$ and band index n, θ is the angle of incidence along $\mathbf{\Gamma}-\mathbf{X}$ and all integrals are calculated over a unit cell with volume V. κ goes from 0 to 1 and measures the strength of coupling to a plane wave of any arbitrary polarization while C_s and C_p measure the overlap between s- and p-polarized plane waves and the Bloch modes. Large reflection for a certain range of angles and frequencies in the absence of band gaps can then be thought of as either a polarization mismatch between the incident wave and the Bloch mode, indicated by small $C_{s/p}$, and/or inefficient mode in-coupling, indicated by small κ.

In Fig. S3, we analyze a slice of the reflection spectrum that corresponds to Bloch modes with momenta $\mathbf{k} = (0.1, 0, k_z)$ $(2\pi/a)$. As previously stated, the band structure weighted by the coupling coefficients shows that there are wavelength ranges where the states are nearly completely s- or p- polarized and/or have small mode coupling index. We particularly point out the wavelength ranges $\sim 4.65 - 4.8$ μm in Fig. S3 (b) and $\sim 5.0 - 5.15$ μm in Fig. S3 (d) (highlighted in blue) which coincide with the sharp increases in reflection. Moreover, the boundary separating the reflecting and transmissive region coincides with band 4 at $k_z = 0$ in s-polarization and band 5 at $k_z = 0$ in p-polarization plots, which are the Weyl bulk bands of interest. Thus the signatures of both bands and the Weyl point are present in simulations and measurements done with 45° polarization.

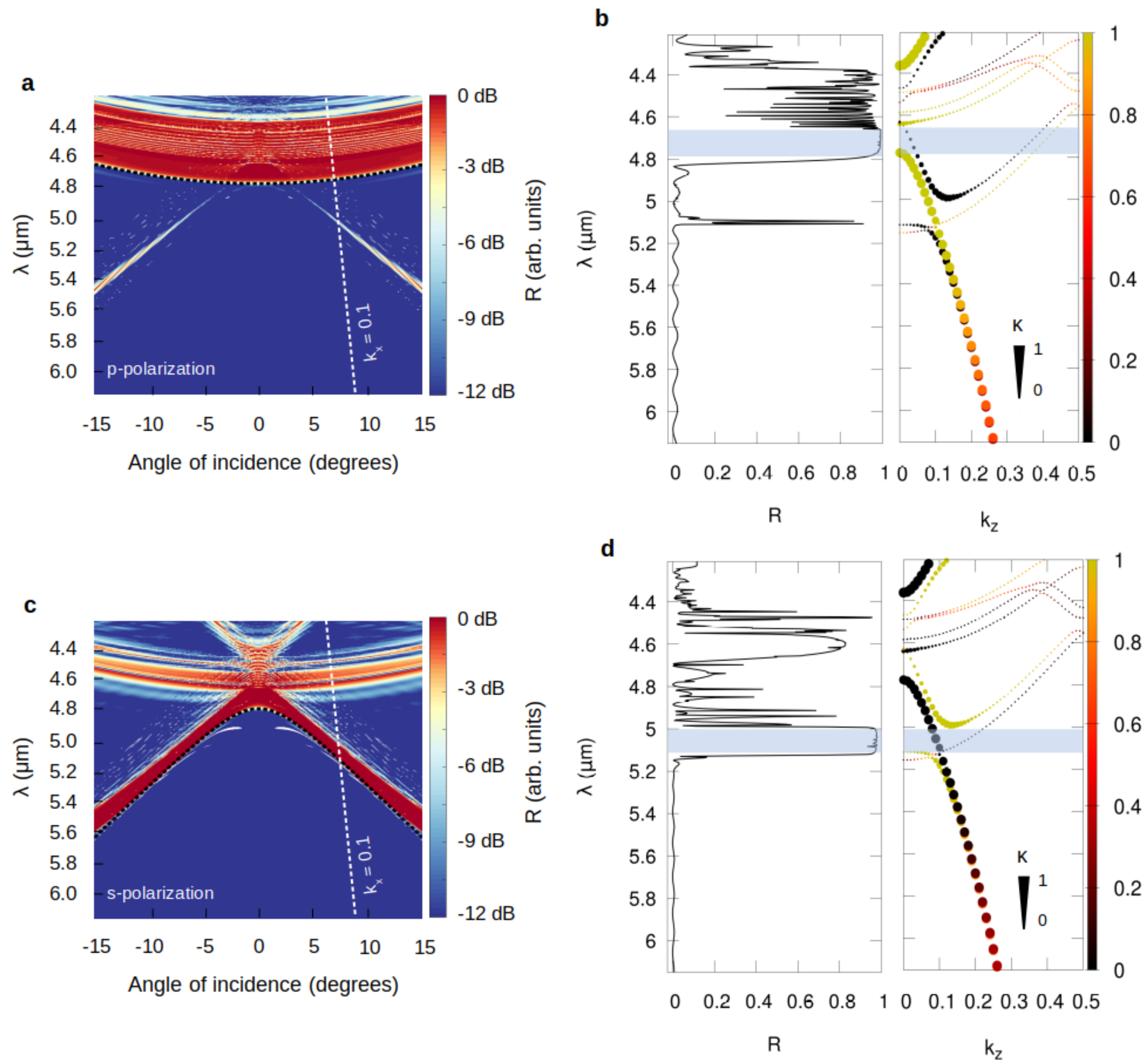

FIG. S3. (a), (c) Angle-resolved RCWA simulation of reflection spectra for p and s polarizations respectively as shown in Fig. 3 of the main text. (b), (d) Reflection spectrum along the cut shown by the dashed line in (a) and (c) and the band structure showing bands 3 to 12 for $\mathbf{k} = (0.1, 0, 0)$ to $(0.1, 0, 0.5)$ $(2\pi/a)$. The color of the circular dots indicates the value of $C_{s/p}$ for the corresponding Bloch modes and their size is proportional to the value of κ.

ADDITIONAL MEASUREMENTS

To provide additional evidence for the robust symmetry protection of the Weyl point, we fabricate and measure another sample with significantly different parameters: rod width of 300 nm and lattice constant of 2.1 μm. Fig S4 shows a SEM image of the sample, along with its transmission spectra. In this case, the transmission measurement was performed using the Hyperion 3000 microscope attached to the FTIR with the in-coupling Cassegrain objective covered except for a small pinhole of 2 mm diameter. This resulted in better k-space resolution for the measurement. We see in Fig. S4 that the charge +2 Weyl point continues to exist, even for these different parameters, and now resides at a wavelength of 2.4 μm.

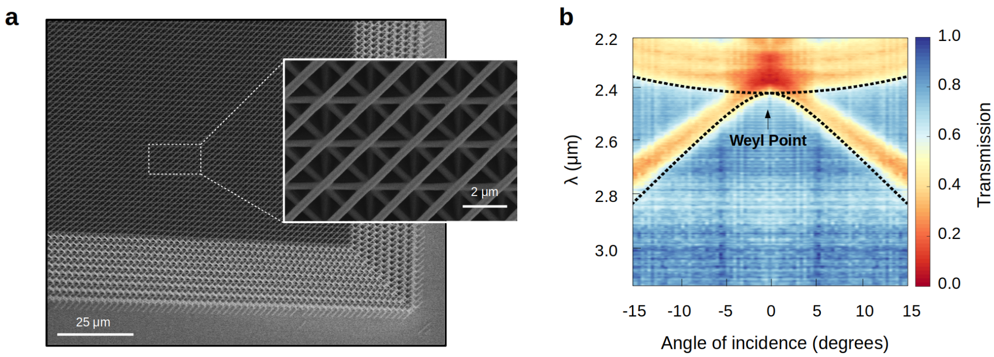

FIG. S4. (a) A SEM image of the chiral woodpile PhC with rod width of 300 nm and lattice constant 2.1 μm. (b) Experimentally measured transmission spectrum in the $\mathbf{\Gamma} - \mathbf{X}$ direction for the PhC shown in (a), overlaid with the bands calculated from MPB shown using black dotted lines.

[1] R. Resta, Journal of Physics: Condensed Matter **12**, R107 (2000).
[2] J. D. Joannopoulos, S. G. Johnson, J. N. Winn, and R. D. Meade, *Photonic Crystals: Molding the Flow of Light*, 2nd ed. (Princeton University Press, 2008).
[3] T.-H. Kao, L.-Y. C. Chien, and Y.-C. Hung, Opt. Express **23**, 24416 (2015).
[4] I. Karakasoglu, M. Xiao, and S. Fan, Opt. Express **26**, 21664 (2018).
[5] M. Saba, M. Thiel, M. D. Turner, S. T. Hyde, M. Gu, K. Grosse-Brauckmann, D. N. Neshev, K. Mecke, and G. E. Schröder-Turk, Phys. Rev. Lett. **106**, 103902 (2011).
[6] S. Takahashi, T. Tajiri, Y. Ota, J. Tatebayashi, S. Iwamoto, and Y. Arakawa, Applied Physics Letters **105**, 051107 (2014).